JCTC Journal of Chemical Theory and Computation

Article

Cite This: J. Chem. Theory Comput. 2019, 15, 4069−4078

pubs.acs.org/JCTC

Assessment of the Linearized *GW* Density Matrix for Molecules

Fabien Bruneval*

DEN, Service de Recherches de Métallurgie Physique, CEA, Université Paris-Saclay, F-91191 Gif-sur-Yvette, France

ABSTRACT: The *GW* approximation is well-known for the calculation of high-quality ionization potentials and electron affinities in solids and molecules. Recently, it has been identified that the density matrix that is obtained from the contraction of the *GW* Green's function allows one to include Feynman diagrams that are significant for the ionization potentials. However, the Green's function contains much more information than the mere quasi-particle energies. Here, we test and assess the quality of this so-called linearized *GW* density matrix for several molecular properties. First of all, we extend the original formulation to perform the linearization starting from any self-consistent mean-field approximation, and not only from Hartree−Fock. We then demonstrate the reliability and the stability of the linearized *GW* density matrix to evaluate the total energy out of a non-self-consistent *GW* calculation. Based on a comprehensive benchmark of 34 molecules, we compare the quality of the electronic density, Hartree energy, exchange energy, and the Fock operator expectation values against other well-established techniques. In particular, we show that the obtained linearized *GW* densities markedly differ from those calculated within the widespread quasi-particle self-consistent *GW* approximation.

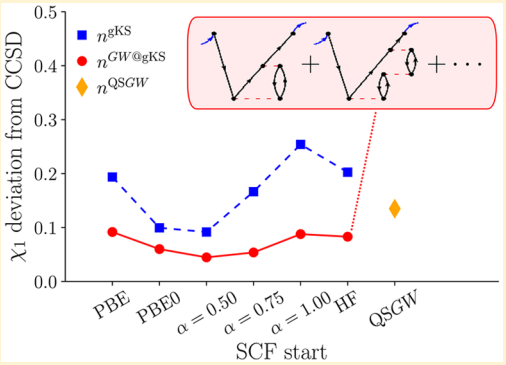

1. INTRODUCTION

The *GW* approximation[1,2] to the self-energy has recently become an accurate and efficient approach to the quasiparticle energies in molecules. These *GW* quasi-particle energies are used either as electron binding energies[3−16] that can be compared to photoemission experiments or as an input for a subsequent Bethe−Salpeter equation calculation of the optical spectra.[17−25] However, once a Green's function is obtained, numerous other molecular properties could be extracted in principle.[26]

For instance, the equal time contraction of the Green's function G gives access to the density matrix γ:

$$\gamma^{\sigma}(\mathbf{r}, \mathbf{r}') = -\mathrm{i}G^{\sigma}(\mathbf{r}t, \mathbf{r}'t^{+}) \tag{1}$$

where σ denotes spin-up or spin-down and t^+ is an abbreviation for the right-hand side limit to t. This density matrix is sufficient to calculate the kinetic energy and the exact-exchange energies.[27] Further contracting the space and spin indexes gives the usual electronic density n:

$$n(\mathbf{r}) = \sum_{\sigma} \gamma^{\sigma}(\mathbf{r}, \mathbf{r}) = -i \sum_{\sigma} G^{\sigma}(\mathbf{r}t, \mathbf{r}t^{+}) \tag{2}$$

which is a direct observable of X-ray diffraction (XRD), for instance.

Despite these attracting features, the Green's function is rarely used to obtain the density matrix or the electronic density, because a diagonal approximation to the self-energy and hence to the Green's function is generally applied.[28,29] A few works go beyond the diagonal approximation when either performing self-consistency,[30,31] obtaining the effective exchange-correlation potential,[32] or evaluating the forces originating from a Green's function.[33]

In our previous work,[34] we had obtained a compact expression for the density matrix that includes some of the *GW* diagrams. We had shown that this density matrix is sufficient to approximate the fully self-consistent *GW* density matrix, thanks to the comparison of the electric dipoles. We had also shown that this *GW* density matrix significantly corrects the Fock operator expectation values, so that the ionization potentials are improved as well. However, these are only two among the many molecular properties that can be obtained from the density matrix itself.

Here, we address the further systematic assessment of this linearized *GW* density matrix. In Section 2, we derive the linearized *GW* density matrix, starting from the Dyson equation in the spin-unrestricted case, and we extend it to a non-Hartree−Fock starting Green's function. In Section 3, we describe the numerical details and study the basis convergence behavior of the density matrix. Total energies, in principle, are beyond the reach of the density matrix. However, in Section 4, we show that the linearized *GW* density matrix are a very useful tool to approach self-consistent *GW* quality total energies. Finally, Section 5 will report an assessment of the linearized *GW* density matrix against other well-established techniques, such as Møller−Plesset perturbation to second-order (MP2)[35] and coupled-cluster methodologies.[36] Hartree atomic units are used throughout the paper.

2. LINEARIZED *GW* DENSITY MATRIX DERIVATION

In the following, we detail a step-by-step derivation of the linearized *GW* density matrix of the formulas published in ref 34.

Received: April 5, 2019
Published: June 13, 2019

DOI: 10.1021/acs.jctc.9b00333
J. Chem. Theory Comput. 2019, 15, 4069−4078

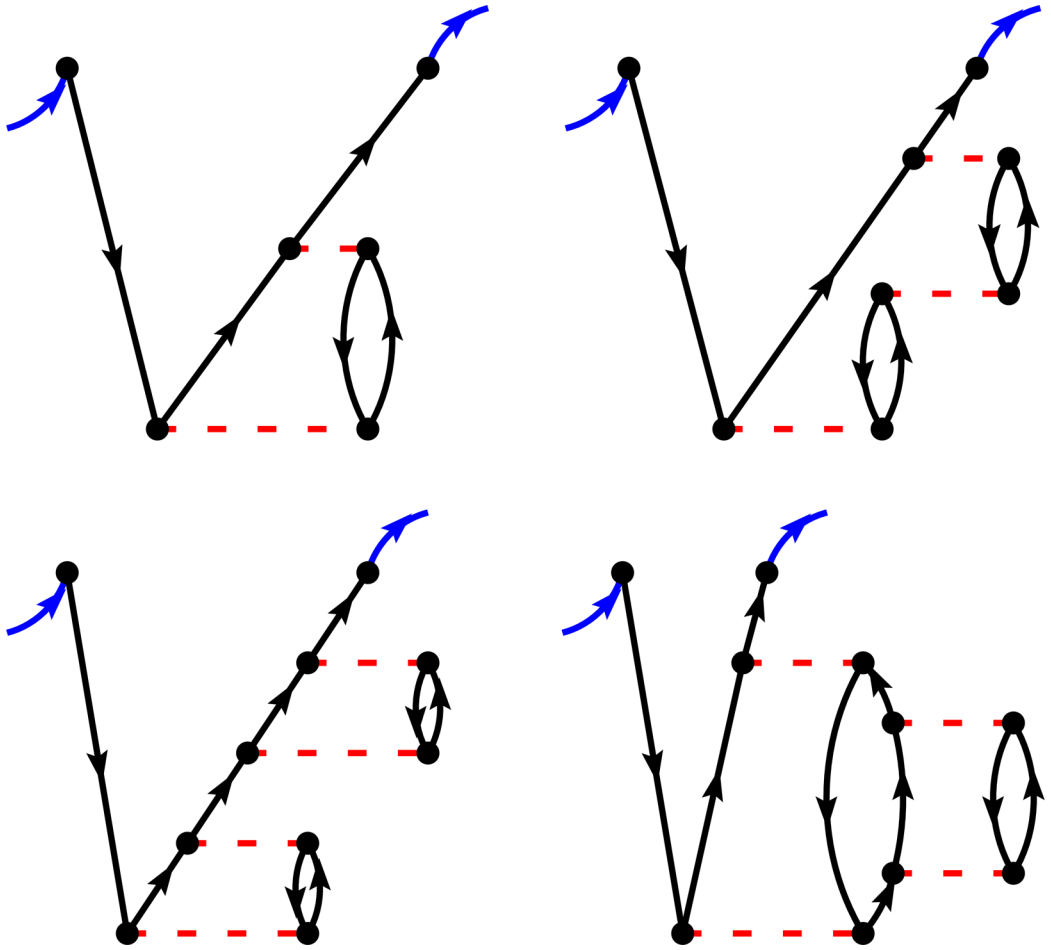

Figure 1. Feynman diagrams for the density matrix, which is simply a Green's function at equal entry and exit times. The noninteracting Green's function are represented as a black arrow and the Coulomb interaction is represented as a horizontal dashed red line. The fully self-consistent *GW* density matrix contains all these diagrams. The two diagrams in the first row are retained in the linearized *GW* density matrix, whereas the two diagrams in the second row are discarded.

Note that Ramberger and co-workers[33] have used the same approximation to the density matrix in the context of force calculations. However, their final expression obtained for imaginary frequencies is more adapted in the context of solids.

Let us start with the Dyson equation for the exact Green's function G with the spin polarization explicitly written:[26]

$$G^\sigma(\mathbf{r}_1 t_1, \mathbf{r}_2 t_2) = G_0^\sigma(\mathbf{r}_1 t_1, \mathbf{r}_2 t_2) + \int \mathrm{d}\mathbf{r}_3 \mathrm{d}\mathbf{r}_4 \mathrm{d}t_3 \mathrm{d}t_4 G_0^\sigma(\mathbf{r}_1 t_1, \mathbf{r}_3 t_3)\Sigma_c^\sigma(\mathbf{r}_3 t_3, \mathbf{r}_4 t_4)G^\sigma(\mathbf{r}_4 t_4, \mathbf{r}_2 t_2) \quad (3)$$

where G_0 represents the Hartree−Fock (HF) Green's function and Σ_c represents the correlation part of the self-energy.

As we focus on the density matrix, we take the limit when the time t_2 is equal to $t_1 + \eta$ (with η being a vanishing positive number), as described in eq 1:

$$\gamma^\sigma(\mathbf{r}_1, \mathbf{r}_2) = \gamma_0^\sigma(\mathbf{r}_1, \mathbf{r}_2) - i \int \mathrm{d}\mathbf{r}_3 \mathrm{d}\mathbf{r}_4 \mathrm{d}t_3 \mathrm{d}t_4 G_0^\sigma(\mathbf{r}_1 t_1, \mathbf{r}_3 t_3)\Sigma_c^\sigma(\mathbf{r}_3 t_3, \mathbf{r}_4 t_4)G^\sigma(\mathbf{r}_4 t_4, \mathbf{r}_2 t_1 + \eta) \quad (4)$$

with γ_0 the HF density matrix.

Let us apply the linearization approximation: all occurrences of the interacting Green's function G on the right-hand side of eq 4 will be replaced with the noninteracting Green's function G_0, as is done in the Sham−Schluter equation context.[37,38]

Then, the correlation part of the self-energy in the *GW* approximation becomes its "one-shot" expression:

$$\Sigma_c^\sigma(\mathbf{r}_3 t_3, \mathbf{r}_4 t_4) = iG_0^\sigma(\mathbf{r}_3 t_3, \mathbf{r}_4 t_4)W_p[G_0](\mathbf{r}_3 t_3, \mathbf{r}_4 t_4) \quad (5)$$

where W_p stands for the polarizable part of the screened Coulomb interaction. W_p contains a dependence on G_0, as is emphasized by the notation $W_\mathrm{p}[G_0]$.

The specific time dependences on the right-hand side of eq 4 call for the use of Fourier transforms:

$$\gamma^\sigma(\mathbf{r}_1, \mathbf{r}_2) = \gamma_0^\sigma(\mathbf{r}_1, \mathbf{r}_2) - \frac{\mathrm{i}}{2\pi} \int \mathrm{d}\mathbf{r}_3 \mathrm{d}\mathbf{r}_4 \mathrm{d}\omega\, \mathrm{e}^{\mathrm{i}\omega\eta} G_0^\sigma(\mathbf{r}_1, \mathbf{r}_3, \omega)\Sigma_c^\sigma(\mathbf{r}_3, \mathbf{r}_4, \omega)G_0^\sigma(\mathbf{r}_4, \mathbf{r}_2, \omega) \quad (6)$$

When finally writing the density matrix γ on the HF eigenstate basis, one obtains the usual density matrix in the molecular orbital basis D that is often used in quantum chemistry:[39]

$$D_{pq\sigma} = \langle p\sigma|\gamma^\sigma|q\sigma\rangle \quad (7)$$

In the mean-field eigenstate basis, G_0 and Σ_c have simple expressions (real-valued wave functions are assumed):[40]

$$G_{0pq}^\sigma = \sum_i \frac{\delta_{pq}\delta_{pi}}{\omega - \epsilon_{i\sigma} - i\eta} + \sum_a \frac{\delta_{pq}\delta_{pa}}{\omega - \epsilon_{a\sigma} + i\eta} \quad (8)$$

DOI: 10.1021/acs.jctc.9b00333
J. Chem. Theory Comput. 2019, 15, 4069−4078

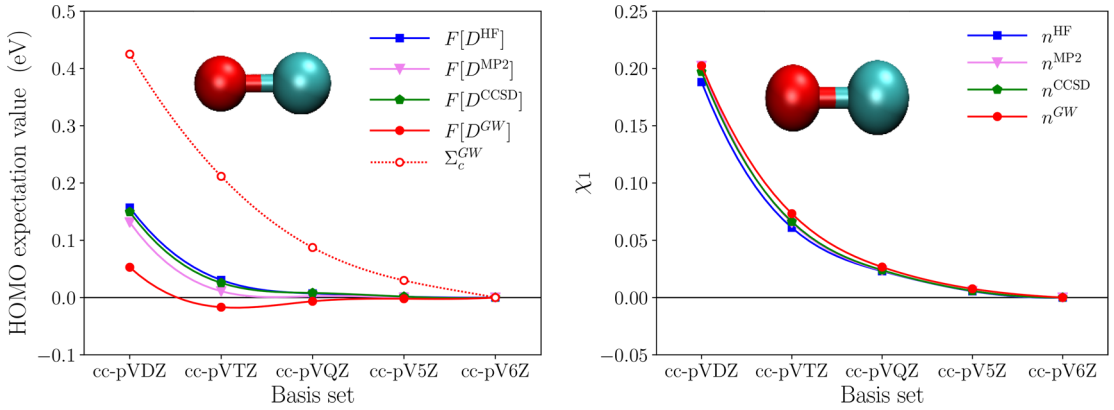

Figure 2. Carbon monoxide basis convergence for Hamiltonian parts in the left-hand panel and for the electronic densities in the right-hand panel. The left-hand panel reports the expectation value of the Fock operator F and the GW self-energy between the HF HOMO wave function. The right-hand panel shows the electronic density difference as measured by the χ_1 distance. The reference in both panels is given by the largest calculation, namely, with the cc-pV6Z basis set.

and

$$\Sigma^{\sigma}_{cpq}(\omega) = \sum_{is} \frac{w^{s}_{pi\sigma} w^{s}_{qi\sigma}}{\omega - \epsilon_{i\sigma} + \Omega_s - i\eta} + \sum_{as} \frac{w^{s}_{pa\sigma} w^{s}_{qa\sigma}}{\omega - \epsilon_{a\sigma} - \Omega_s + i\eta} \tag{9}$$

where, here and in the following, indexes i, j run over occupied states, indexes a, b run over unoccupied states, and indexes p, q run over all the states. The index s enumerates the neutral excitation energies Ω_s and their coefficients $w^{s}_{mi\sigma}$. These quantities can be obtained through the diagonalization of the random-phase approximation (RPA) equation[40,41] (similar to the Casida equation[42]).

The residue theorem allows one to perform the ω-integral in eq 6 for the different occupation cases and yields the final result for the linearized GW density matrix D^{GW}:

$$D^{GW}_{ij\sigma} = \delta_{ij} - \sum_{as} \frac{w^{s}_{ia\sigma} w^{s}_{ja\sigma}}{(\epsilon_{i\sigma} - \epsilon_{a\sigma} - \Omega_s)(\epsilon_{j\sigma} - \epsilon_{a\sigma} - \Omega_s)} \tag{10a}$$

$$D^{GW}_{ab\sigma} = -\sum_{is} \frac{w^{s}_{ai\sigma} w^{s}_{bi\sigma}}{(\epsilon_{i\sigma} - \epsilon_{a\sigma} - \Omega_s)(\epsilon_{i\sigma} - \epsilon_{b\sigma} - \Omega_s)} \tag{10b}$$

$$D^{GW}_{ib\sigma} = \frac{1}{\epsilon_{i\sigma} - \epsilon_{b\sigma}} \left[\sum_{as} \frac{w^{s}_{ia\sigma} w^{s}_{ba\sigma}}{(\epsilon_{i\sigma} - \epsilon_{a\sigma} - \Omega_s)} - \sum_{js} \frac{w^{s}_{ij\sigma} w^{s}_{bj\sigma}}{(\epsilon_{j\sigma} - \epsilon_{b\sigma} - \Omega_s)} \right] \tag{10c}$$

This result is identical to the one reported in ref 34, except that it is generalized to the spin-unrestricted case.

The expression for the linearized GW density matrix D^{GW} is rather compact. This relative simplicity could only be obtained because of the linearization approximation. However, it comes at the expense of neglecting some contributions. Figure 1 reports an illustrative subset of the Feynman diagrams contained in the fully self-consistent GW density matrix. The GW approximation contains the series of ring diagrams that account for non-interacting electron−hole pairs. The subsequent ring diagrams in the first row of Figure 1 are already included at the "one-shot" GW level. Then, when solving the Dyson equation, subsequent sequences of the "one-shot" GW self-energy are inserted as in the diagram in the lower left-hand corner. Moreover, when performing self-consistent GW calculation, the Green's function itself contains "one-shot" GW self-energy additions, as exemplified in the lower right-hand corner. In the linearized density matrix, the Dyson equation is not inverted and the self-consistency is not performed; therefore, only the diagrams in the first row are retained.

This simplification has positive consequences on the computation burden. Let us consider the case of a growing cluster made of identical atoms, each atom being described with a constant number of basis functions. The number of occupied states and the number of empty states both scale as N, where N is the number of atoms. The index s running over the neutral excitations is proportional to N^2 (occupied-to-empty and empty-to-occupied transitions). The overall computational scaling of Eqs. 10a−10c then is N^5. In *canonical* GW local basis implementations,[40,41,43,44] the actual bottleneck would remain in the diagonalization of the RPA equation anyway, since this operation scales as N^6. The *canonical* implementation is certainly the simplest and the fastest for small systems. But there exists alternate expressions that formally offer a better scaling and that may become competitive for larger systems. For instance, by inserting the Resolution-of-the-Identity approximation and evaluating the functions for imaginary frequencies,[33,45] one can show that the scaling is decreased down to N^4.

For the sake of simplicity, we have limited our derivation to a HF Green's function in the Dyson equation shown in eq 3. In this study, our focus is on testing other starting Green's functions and, in particular, coming from the generalized Kohn−Sham approach. Such a starting point violates the Brillouin theorem,[46,47] and first-order corrections to the self-energy and then to the Green's function are to appear. We can extend the previous HF-based derivation by considering the following linearized Dyson equation:

$$G = G_{\mathrm{gKS}} + G_{\mathrm{gKS}}(\Sigma_x + \Sigma_c - V_{xc})G_{\mathrm{gKS}} \tag{11}$$

where indexes have been dropped for the sake of simplicity. Σ_x is the exact-exchange operator and V_{xc} is the generalized Kohn−Sham potential, which can be either local or nonlocal.

The Σ_c term in eq 11 yields the linearized GW density matrix of eqs 10a−10c, but with generalized Kohn−Sham eigenener-

DOI: 10.1021/acs.jctc.9b00333
J. Chem. Theory Comput. 2019, 15, 4069−4078

gies and eigenstates. The $\Sigma_x - V_{xc}$ term generates a rather simple additional contribution to the density matrix:

$$\Delta D_{ib\sigma}^{\text{non-Brillouin}} = \frac{1}{\epsilon_{i\sigma} - \epsilon_{b\sigma}} \langle i\sigma | \Sigma_x^\sigma - V_{xc}^\sigma | b\sigma \rangle \tag{12}$$

This term only affects the occupied-virtual and virtual-occupied blocks in the state representation of D. In the following, this term is included each time the starting-point Green's function is not HF.

3. TECHNICALITIES AND BASIS SET CONVERGENCE

The linearized *GW* density matrix reported in eqs 10a−10c, and its non-Brillouin correction in eq 12, have been implemented in the Gaussian basis code MOLGW.[40] In the following, we employ the Dunning correlation-consistent basis family.[48] Although not necessary, the results reported hereafter all use the Resolution-of-the-Identity approximation with the auxiliary basis sets developed by Weigend.[49] In addition, the core states have been excluded from the summations: this is a frozen core approximation that is very well-justified for *GW*.[10] The reference density matrices obtained within the coupled cluster limited to single and double excitations (CCSD) and MP2 have been extracted from Gaussian16[50] and then read by MOLGW for the post-treatment. To facilitate the communication between the two codes, we chose to employ Cartesian Gaussian functions instead of the solid harmonics that one, in principle, should use with the original Dunning basis sets.[48]

In the following sections, we probe the effect of the starting point by tuning a hybrid exchange-correlation functional. We will examine the α and β parameters in the energy functional,

$$E_{xc} = \alpha E_x[\gamma^\sigma] + (1-\alpha) E_x^{\text{PBE}}(n^\sigma, \nabla n^\sigma) + \beta E_c^{\text{PBE}}(n^\sigma, \nabla n^\sigma) \tag{13}$$

where $E_x[\gamma]$ is the usual exact-exchange energy, E_x^{PBE} is the PBE exchange, and E_c^{PBE} is the correlation generalized gradient approximation to the density functional theory.[51] This functional form is flexible enough to span a wide range of representative functionals: using $\alpha = 1$ and $\beta = 0$ yields HF, $\alpha = 0$ and $\beta = 1$ gives PBE, $\alpha = 0.25$ and $\beta = 1$ gives PBE0.[52]

One might be concerned about the convergence of the linearized *GW* density matrix, when one knows about the notoriously slow convergence of the *GW* self-energy on a localized basis.[10] We exemplify this statement with the *GW* self-energy evaluated for the highest occupied molecular orbital (HOMO) of carbon monoxide in the left-hand panel of Figure 2. The smallest basis set, namely, cc-pVDZ, deviate by more than 0.4 eV, with respect to the largest basis set. The situation is much nicer for the Fock operator F evaluated with the linearized *GW* density matrix. The basis set dependence of $F[D^{GW}]$ is even weaker than that observed with the other density matrices. The smallest basis set already gives an estimate of the converged Fock expectation value within 50 meV.

The right-hand panel of Figure 2 shows an alternate measure of the density matrix convergence by measuring the difference between the resulting electronic densities. We introduce the χ_1 distance between two electronic densities following the work of Caruso et al.:[53]

$$\chi_1^{\text{AB}} = \int d\mathbf{r} |n^{\text{A}}(\mathbf{r}) - n^{\text{B}}(\mathbf{r})| \tag{14}$$

In practice, we perform the integral in eq 14 on the same dense real-space grid as the one used to evaluate the exchange-correlation potential of density functional theory (DFT).[40] The right-hand panel of Figure 2 shows that the linearized *GW* electronic density convergence is consistent with the other expressions.

As a conclusion, the slow convergence of the *GW* self-energy does not permeate to the linearized *GW* density matrix. This positive statement may open the way for the calculation of large systems with reasonable basis sets, softening the N^5 scaling reported in Section 2.

4. AN ALTERNATE *GW* TOTAL ENERGY FUNCTIONAL

The total energy corresponding to the *GW* self-energy is not uniquely defined when not evaluated self-consistently.[55−57] Indeed, the total energy can be obtained from the Galitskii−Migdal formula,[58] from the Klein or Pines functional[59,60] (which corresponds to the RPA formula in the adiabatic connection framework) or from the Luttinger−Ward functional.[61] However, these functionals are only a subset of an infinite number of possibilities. In the early 2000, Dahlen and co-workers[56,62,63] published a series of papers to evaluate the different functionals. Their primary purpose was to elucidate which total energy functional is best-suited for an inexpensive non-self-consistent evaluation. This amounts to the quest of the functional form that shows the weakest dependence, with respect to the input Green's function. Among those functionals, the RPA functional has gained noticeable popularity in chemistry and physics, because of its relatively low computational cost and its weaker dependence on the starting point.[64−69]

In this section, we examine whether the improved density matrix can help in designing a more stable total energy functional. Indeed, many contributions to the total energy are direct functionals of the density matrix. The HF energy (E_{HF}) that contains the kinetic energy, the electron−nucleus attraction, the Hartree energy, and the exact exchange energies can be obtained directly from the density matrix:

$$T[\gamma] = \sum_\sigma \int d\mathbf{r} \lim_{\mathbf{r}' \to \mathbf{r}} \left[-\frac{\nabla_{\mathbf{r}'}^2}{2} \gamma^\sigma(\mathbf{r}, \mathbf{r}') \right] \tag{15a}$$

$$E_{\text{ext}}[\gamma] = \sum_\sigma \int d\mathbf{r}\, v_{\text{ext}}(\mathbf{r}) \gamma^\sigma(\mathbf{r}, \mathbf{r}) \tag{15b}$$

$$E_H[\gamma] = \frac{1}{2} \sum_{\sigma\sigma'} \int d\mathbf{r}\, d\mathbf{r}' \frac{\gamma^\sigma(\mathbf{r}, \mathbf{r}) \gamma^{\sigma'}(\mathbf{r}', \mathbf{r}')}{|\mathbf{r} - \mathbf{r}'|} \tag{15c}$$

$$E_x[\gamma] = -\frac{1}{2} \sum_\sigma \int d\mathbf{r}\, d\mathbf{r}' \frac{\gamma^\sigma(\mathbf{r}, \mathbf{r}') \gamma^\sigma(\mathbf{r}', \mathbf{r})}{|\mathbf{r} - \mathbf{r}'|} \tag{15d}$$

$$E_{\text{HF}}[\gamma] = T[\gamma] + E_{\text{ext}}[\gamma] + E_H[\gamma] + E_x[\gamma] \tag{15e}$$

The only contribution missing is the correlation energy, which depends on the complete Green's function. The *GW* correlation energy can be written as[57]

$$E_c^{GW}[G] = \frac{1}{2} \int_{-\infty}^{+\infty} \frac{d\nu}{2\pi} \int d\mathbf{r}_1 d\mathbf{r}_2 \frac{1}{|\mathbf{r}_1 - \mathbf{r}_2|} \times [\chi^1(\mathbf{r}_2, \mathbf{r}_1, i\nu) - \chi^0(\mathbf{r}_2, \mathbf{r}_1, i\nu)] \tag{16}$$

where the integration over the imaginary frequencies $i\nu$ is more convenient. The interacting (noninteracting) density−density responses have been introduced with the notation χ^1 (χ^0). It can be shown that this term can also be written as $^1/_2\,\text{Tr}[\Sigma_c G]$.

DOI: 10.1021/acs.jctc.9b00333
J. Chem. Theory Comput. 2019, 15, 4069−4078

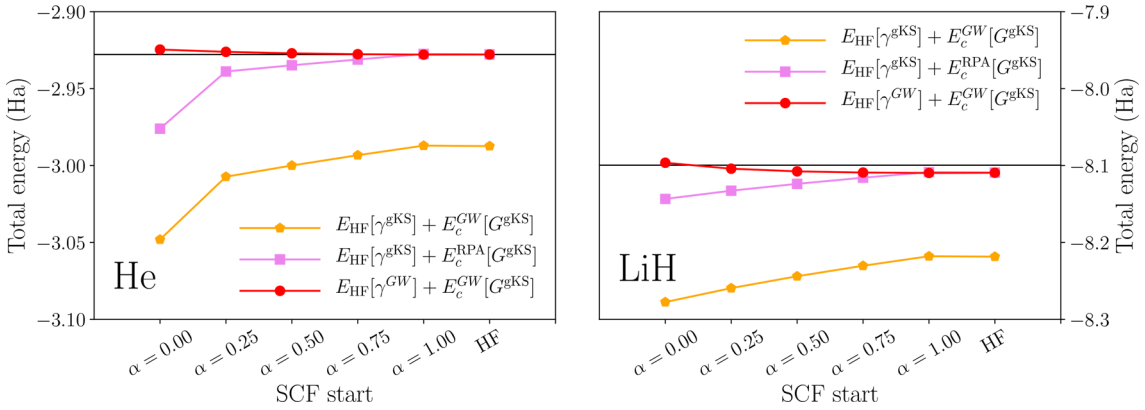

Figure 3. Total energy as a function of the starting point for two finite systems: a He atom (left-hand panel) and a LiH molecule (right-hand panel). The LiH bond length is close to equilibrium with $r = 3.035$ Bohr. The horizontal line represents the self-consistent *GW* total energies published by Stan et al.[54]

Using the adiabatic switching-on of the Coulomb interaction, one can integrate over λ from 0 (noninteracting) to 1 (fully interacting) and obtain an alternate expression for the correlation energy in the case of a noninteracting Green's function, the Klein functional:

$$E_c^{\text{Klein}}[G] = \frac{1}{2}\int_0^1 d\lambda \int_{-\infty}^{+\infty} \frac{d\nu}{2\pi} \int d\mathbf{r}_1 d\mathbf{r}_2 \frac{1}{|\mathbf{r}_1 - \mathbf{r}_2|} \times [\chi^\lambda(\mathbf{r}_2, \mathbf{r}_1, i\nu) - \chi^0(\mathbf{r}_2, \mathbf{r}_1, i\nu)] \quad (17)$$

where the scaled density−density response function χ^λ is obtained from a Dyson-like equation:

$$\chi^\lambda(\mathbf{r}_1, \mathbf{r}_2, i\nu) = \chi^0(\mathbf{r}_1, \mathbf{r}_2, i\nu) + \int d\mathbf{r}_3 d\mathbf{r}_4 \chi^0(\mathbf{r}_1, \mathbf{r}_3, i\nu) \frac{\lambda}{|\mathbf{r}_3 - \mathbf{r}_4|} \chi^\lambda(\mathbf{r}_4, \mathbf{r}_2, i\nu) \quad (18)$$

Finally, the noninteracting density−density response function is obtained from the Green's function itself:

$$\chi^0(\mathbf{r}_1, \mathbf{r}_2, i\nu) = -\int_{-\infty}^{+\infty} \frac{d\nu'}{2\pi} G(\mathbf{r}_1, \mathbf{r}_2, i\nu) G(\mathbf{r}_2, \mathbf{r}_1, i\nu + i\nu') \quad (19)$$

where the dependence of the correlation energy on G is made obvious.

The difference between the *GW* correlation energy in eq 16 and the Klein correlation energy in eq 17 comes from the fact that the latter contains the correlated kinetic energy, whereas the former does not.[57,70]

In Figure 3, we compare the sensitivity of the total energy functionals to the starting point when evaluated for a noninteracting Green's function for two finite systems: He and LiH. For noninteracting Green's function, the Klein functionals reduces to the usual RPA functional. We will name it RPA from now on. The orange line represents the Galitskii−Migdal formula, using a mean-field starting point G_{gKS}. The pink line shows the RPA total energy. The red line is an alternate proposition: Evaluate the HF energy part with the linearized *GW* density matrix and combine it with the *GW* correlation energy E_c^{GW}:

$$E_{GW}[G_{in}] = E_{HF}[G_{gKS} + G_{gKS}(\Sigma_x + \Sigma_c - V_{xc})G_{in}] + \frac{1}{2}\text{Tr}[\Sigma_c G_{in}] \quad (20)$$

When inserting the self-consistent *GW* Green's function in eq 20, one recovers the usual Galitskii−Migdal expression for the total energy. When inserting $G_{in} = G_{gKS}$, the argument of the HF energy becomes the linearized *GW* density matrix that we introduced in the previous sections.

The trace of the density matrix (i.e., the sum of the eigenvalues) yields the number of electrons. We have numerically verified, on several molecules, that the number of electrons obtained from the linearized *GW* density matrix is conserved to the machine precision. This contrasts with the nonlinearized Dyson equation, using the "one-shot" *GW* self-energy that is known to violate the particle number conservation.[54,71] This particle number conservation is an important prerequisite when evaluating total energies.

According to Figure 3, the stability of the proposed *GW* total energy functional (shown in red in the figure) is much superior to that of the Galitskii−Migdal formula, but also is superior to that of the RPA functional. The sensitivity to the amount of exact exchange α in the input Green's function is ∼3 times weaker in the functional of eq 20, compared to RPA. These total energies compare well with the self-consistent *GW* energies obtained by Stan et al.,[54] although it is difficult to compare the absolute numbers, because of the use of different basis sets. In our work, we use very accurate basis sets: cc-pV6Z for He and cc-pCVQZ for LiH. Note that the core polarization basis functions for the Li 1*s* orbital were absolutely needed to approach the values reported by Stan et al.[54]

In Appendix A, we show the agreement between the natural occupation numbers obtained from the linearized *GW* density matrix and the fully self-consistent *GW* density matrix. We show, in particular, that the obtained density matrix is not idempotent.

As a conclusion, the use of the linearized *GW* density matrix that readily contains the correlated kinetic energy yields a very stable total energy. This expression requires only one evaluation of W, which is generally the bottleneck in *GW* calculations and, hence, is much lighter than a fully self-consistent calculation.

5. BENCHMARK AGAINST CCSD DENSITY MATRICES

In this section, we evaluate the performance of the linearized density matrix itself. To do so, we consider a standard benchmark of 34 small molecules[4,10,34] for which coupled-cluster density matrices (in the CCSD approximation) have been obtained. The molecules of the benchmark are all closed-shell. They contain 10 different elements and have different

DOI: 10.1021/acs.jctc.9b00333
J. Chem. Theory Comput. 2019, 15, 4069−4078

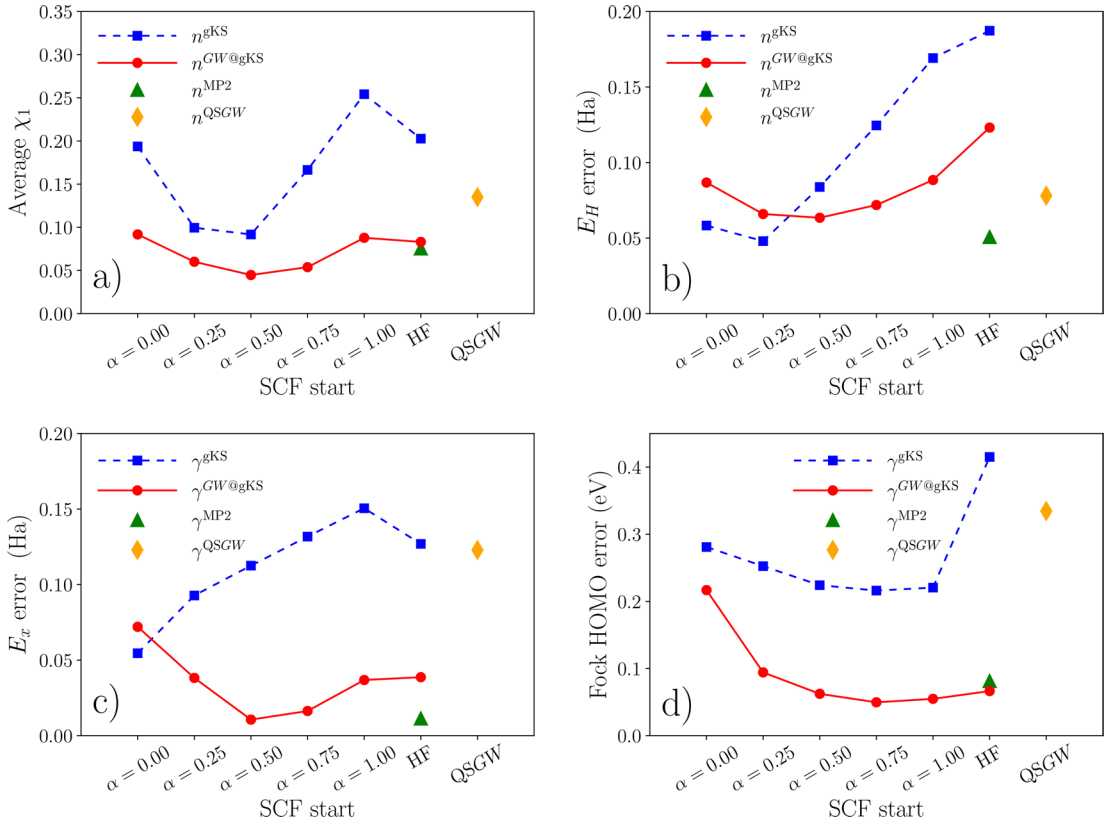

Figure 4. Average error, with respect to CCSD, across a benchmark of 34 molecules (the average error induced by an approximated density matrix is plotted as a function of the starting point): (a) evaluates the deviation through the χ_1 measure on the electronic density, (b) evaluates the deviation through the error on the Hartree energy E_H, (c) evaluates the deviation through the exchange energy E_x, and (d) evaluates the deviation through the HOMO expectation value of the Fock operator. The expectation value is performed between a constant PBE0 HOMO wave function.

types of bonding: from covalent (with single, double, and triple bonds) to ionic bonds. We used the same Cartesian cc-pVQZ basis for all of the calculations. Note that the limitation in the size of the molecules considered here only comes from the limitation in the CCSD density matrix calculations. The linearized *GW* density matrix is computationally much more favorable and does not require the solution of the Z-vector equation.[72−74]

There is no unique way to evaluate the difference between two density matrices. In the following, we have selected four different measures for the deviation with respect to the CCSD density matrix, as shown in Figure 4. The data gathered in Figure 4 are averaged over the entire set of molecules. In Appendix B, we provide, as an illustration, individual results for a representative subset of the data. First, in Figure 4a, we consider the χ_1 difference in the electronic densities, as defined in eq 14. This measure is equally weighted in all space. The Hartree energy difference reported in Figure 4b is also only sensitive to the electronic density, but more weight is given where the electronic density is larger (see eq 15c). The exchange energy in Figure 4c is similar but sensitive to the density matrix itself and is not only sensitive to the electronic density (see eq 15d). Finally, Figure 4d) also reports the Fock operator expectation value on the HOMO orbital, since it is the relevant quantity in the calculation for an ionization potential calculation. Note that the HOMO orbital is kept constant to the PBE0 HOMO orbital in order to be able to compare the different density matrices.

Whatever the retained criterium in Figure 4, the generalized Kohn−Sham density matrices always perform the worst, with respect to CCSD. The PBE and PBE0 are not surprisingly the ones that minimize the error among those. The linearized *GW* density matrices are a huge improvement over the generalized Kohn−Sham ones. They are much less sensitive to the starting point. In our previous work,[34] we only considered a HF starting point. Here, by correctly including the first-order correction given in eq 12, we could generalize to any starting point. From Figure 4, we conclude that the hybrid functional starting point with $\alpha \approx 50\%$ produce the most accurate results for χ_1, E_H, and E_x. The best starting point for the Fock operator is obtained with $\alpha \approx 75\%$, which is not much different. The linearized *GW* results have about the same quality as the MP2 density matrix, but without the need to solve the cumbersome Z-vector equation.

As already stated above, obtaining the self-consistent *GW* electronic density or quasi-particle wave functions is tedious. To circumvent this problem, Kotani and van Schilfgaarde proposed a clever static approximation to the *GW* self-energy: the quasi-particle self-consistent *GW* approximation (QSGW):[75,76]

$$\Sigma^{\mathrm{QSGW}}_{cpq\sigma} = \frac{1}{4}[\Sigma^{\sigma}_{cpq}(\epsilon_{p\sigma}) + \Sigma^{\sigma}_{cqp}(\epsilon_{p\sigma}) + \Sigma^{\sigma}_{cpq}(\epsilon_{q\sigma}) + \Sigma^{\sigma}_{cqp}(\epsilon_{q\sigma})] \tag{21}$$

This approximation has been applied successfully for solids[30,77−79] and for molecules.[6,11,53,80−82]

Since QSGW is an approximation to the fully self-consistent *GW* scheme, its electronic density and its density matrix may depart from the fully self-consistent ones.[53] Figure 4 also includes the errors of QSGW with respect to CCSD. QSGW approximation shows rather large deviations. Generally, it does

DOI: 10.1021/acs.jctc.9b00333
J. Chem. Theory Comput. 2019, 15, 4069−4078

not perform as well as the linearized *GW* density matrix. Its quality is comparable to that of PBE0.

To evaluate how different QSGW and D^{GW} are, let us compare the χ_1 distance between QSGW, CCSD, and $D^{\mathrm{GW@PBE0}}$. Unexpectedly, we obtain a greater distance between QSGW and $D^{\mathrm{GW@PBE0}}$, with $\chi_1 = 0.17$ than the distance between QSGW and CCSD ($\chi_1 = 0.13$), and than the distance between $D^{\mathrm{GW@PBE0}}$ and CCSD ($\chi_1 = 0.06$). As a conclusion, QSGW and the linearized *GW* density matrix differ noticeably, even though they are both supposed to be approximations to self-consistent *GW*.

6. CONCLUSION

The spin-unrestricted expression for the linearized *GW* density matrix has been derived in the molecular orbital basis. This expression is compact with a computational scaling in N^5, which is anyway more favorable than the canonical calculation of the screened Coulomb interaction W in N^6. It can be implemented straightforwardly in a localized orbital *GW* code. The convergence behavior of the linearized *GW* density matrix is much faster than that of the slow convergence to which one is accustomed with the *GW* self-energy. We have generalized the original derivation to any generalized Kohn−Sham starting Green's function.

The linearized *GW* density matrix allows one to recalculate all of the terms in the total energy except the correlation energy. Combining these updated terms with the *GW* correlation energy yields a total energy expression that approaches well the fully self-consistent *GW* energy. The obtained results are less sensitive to the input Green's function than the commonly used RPA functional.

The quality of the linearized *GW* density matrix has then been assessed using a large benchmark (34 molecules), for which reference CCSD density matrices could be calculated. The quality of linearized *GW* density matrix is improved by tuning the initial mean-field approximation, and we found that hybrid functionals with a high content of exchange (50%−75%) are best. The final quality of the density matrix is similar to that of MP2, but without having to solve the cumbersome Z-vector equation. Furthermore, the computational scaling could be reduced in the future by switching to an imaginary frequency implementation. Surprisingly, the density matrix obtained from QSGW is much different from the linearized *GW* one and, generally, is of poorer quality.

This assessment of the linearized *GW* density matrix is a necessary step toward a broad use of this handy and accurate approximation. It opens the possibility of using larger molecules or condensed matter systems.

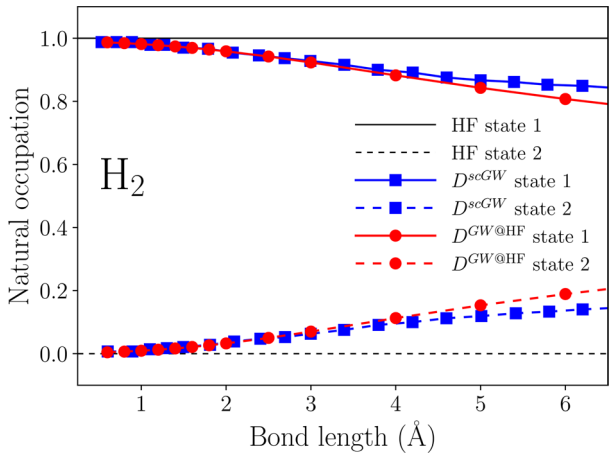

Figure A-1. Natural occupation numbers for the two most occupied states in H_2, as a function of the bond length. The fully self-consistent *GW* result are extracted from ref 57.

APPENDIX A

Natural Occupation Numbers in H_2 Dissociation

The calculation of a density matrix allows one to obtain natural occupation numbers that are the eigenvalues of this density matrix. In ref 57, Hellgren et al. have evaluated the self-

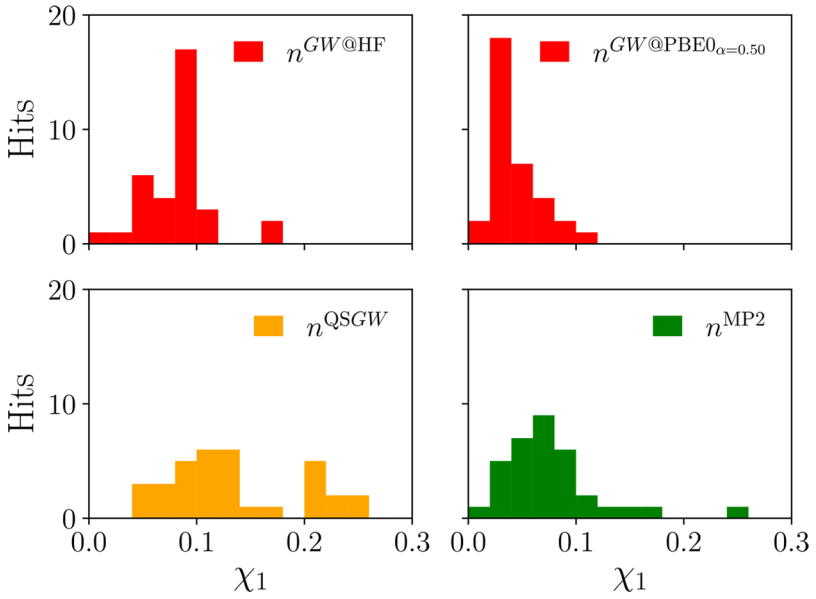

Figure B-1. χ_1 error distribution accross a benchmark of 34 molecules. The references are CCSD electronic densities. Four different approximations have been selected as illustrative examples: the linearized *GW* density matrix based on HF, the linearized *GW* based on an hybrid functional with 50% of exact exchange, QSGW, and MP2.

DOI: 10.1021/acs.jctc.9b00333
J. Chem. Theory Comput. 2019, 15, 4069−4078

consistent *GW* natural occupation numbers as a function of the streching of the H_2 molecule. In Figure A-1, we have reproduced the calculations of ref 57, but using the linearized *GW* density matrix. The linearized *GW* density matrix based on HF matches the outcome of the self-consistent *GW* very closely. This is another successful test for the linearized *GW* density matrix.

APPENDIX B

χ_1 Error Distribution of the Electronic Density in the 34 Molecule Benchmark

Figure B-1 shows some of the data used to produce the panel a) of Figure 4. The error in the electronic density is quantified with the χ_1 measure as defined in eq 14. The references are given by CCSD calculations. The linearized *GW* density matrices produce rather regular distributions of error. QSGW shows a flatter distribution with many outliers: C_2H_2, C_2H_4, F_2, Na_2, N_2, CO_2 have a χ_1 larger than 0.20. MP2 has a low average error with a single outlier: SO_2.

AUTHOR INFORMATION

Corresponding Author

*E-mail: fabien.bruneval@cea.fr.

ORCID

Fabien Bruneval: 0000-0003-0885-8960

Notes

The author declares no competing financial interest.

ACKNOWLEDGMENTS

This work was performed using HPC resources from GENCI-CCRT (Grant No. 2019-gen6018).

REFERENCES

(1) Hedin, L. New Method for Calculating the One-Particle Green's Function with Application to the Electron-Gas Problem. *Phys. Rev.* **1965**, *139*, A796−A823.

(2) Reining, L. The GW approximation: content, successes and limitations. *Wiley Interdiscip. Rev.: Comput. Mol. Sci.* **2018**, *8*, e1344.

(3) Grossman, J. C.; Rohlfing, M.; Mitas, L.; Louie, S. G.; Cohen, M. L. High Accuracy Many-Body Calculational Approaches for Excitations in Molecules. *Phys. Rev. Lett.* **2001**, *86*, 472−475.

(4) Rostgaard, C.; Jacobsen, K. W.; Thygesen, K. S. Fully self-consistent GW calculations for molecules. *Phys. Rev. B: Condens. Matter Mater. Phys.* **2010**, *81*, 085103.

(5) Blase, X.; Attaccalite, C.; Olevano, V. First-principles GW calculations for fullerenes, porphyrins, phtalocyanine, and other molecules of interest for organic photovoltaic applications. *Phys. Rev. B: Condens. Matter Mater. Phys.* **2011**, *83*, 115103.

(6) Bruneval, F. Ionization energy of atoms obtained from GW self-energy or from random phase approximation total energies. *J. Chem. Phys.* **2012**, *136*, 194107.

(7) Ren, X.; Rinke, P.; Blum, V.; Wieferink, J.; Tkatchenko, A.; Sanfilippo, A.; Reuter, K.; Scheffler, M. Resolution-of-identity approach to Hartree−Fock, hybrid density functionals, RPA, MP2 and GW with numeric atom-centered orbital basis functions. *New J. Phys.* **2012**, *14*, 053020.

(8) Sharifzadeh, S.; Tamblyn, I.; Doak, P.; Darancet, P.; Neaton, J. Quantitative molecular orbital energies within a G0W0 approximation. *Europ. Phys. J. B* **2012**, *85*, 323.

(9) Körzdörfer, T.; Marom, N. Strategy for finding a reliable starting point for G_0W_0 demonstrated for molecules. *Phys. Rev. B: Condens. Matter Mater. Phys.* **2012**, *86*, 041110.

(10) Bruneval, F.; Marques, M. A. L. Benchmarking the Starting Points of the GW Approximation for Molecules. *J. Chem. Theory Comput.* **2013**, *9*, 324−329.

(11) Koval, P.; Foerster, D.; Sánchez-Portal, D. Fully self-consistent GW and quasiparticle self-consistent GW for molecules. *Phys. Rev. B: Condens. Matter Mater. Phys.* **2014**, *89*, 155417.

(12) van Setten, M. J.; Caruso, F.; Sharifzadeh, S.; Ren, X.; Scheffler, M.; Liu, F.; Lischner, J.; Lin, L.; Deslippe, J. R.; Louie, S. G.; Yang, C.; Weigend, F.; Neaton, J. B.; Evers, F.; Rinke, P. GW100: Benchmarking G0W0 for Molecular Systems. *J. Chem. Theory Comput.* **2015**, *11*, 5665−5687.

(13) Govoni, M.; Galli, G. Large Scale GW Calculations. *J. Chem. Theory Comput.* **2015**, *11*, 2680−2696.

(14) Knight, J. W.; Wang, X.; Gallandi, L.; Dolgounitcheva, O.; Ren, X.; Ortiz, J. V.; Rinke, P.; Körzdörfer, T.; Marom, N. Accurate Ionization Potentials and Electron Affinities of Acceptor Molecules III: A Benchmark of GW Methods. *J. Chem. Theory Comput.* **2016**, *12*, 615−626.

(15) Maggio, E.; Liu, P.; van Setten, M. J.; Kresse, G. GW100: A Plane Wave Perspective for Small Molecules. *J. Chem. Theory Comput.* **2017**, *13*, 635−648.

(16) Lange, M. F.; Berkelbach, T. C. On the Relation between Equation-of-Motion Coupled-Cluster Theory and the GW Approximation. *J. Chem. Theory Comput.* **2018**, *14*, 4224−4236.

(17) Onida, G.; Reining, L.; Godby, R. W.; Del Sole, R.; Andreoni, W. *Ab Initio* Calculations of the Quasiparticle and Absorption Spectra of Clusters: The Sodium Tetramer. *Phys. Rev. Lett.* **1995**, *75*, 818−821.

(18) Rohlfing, M.; Louie, S. G. Optical Excitations in Conjugated Polymers. *Phys. Rev. Lett.* **1999**, *82*, 1959−1962.

(19) Blase, X.; Attaccalite, C. Charge-transfer excitations in molecular donor-acceptor complexes within the many-body Bethe-Salpeter approach. *Appl. Phys. Lett.* **2011**, *99*, 171909.

(20) Jacquemin, D.; Duchemin, I.; Blase, X. Benchmarking the Bethe−Salpeter Formalism on a Standard Organic Molecular Set. *J. Chem. Theory Comput.* **2015**, *11*, 3290−3304.

(21) Bruneval, F.; Hamed, S. M.; Neaton, J. B. A systematic benchmark of the ab initio Bethe-Salpeter equation approach for low-lying optical excitations of small organic molecules. *J. Chem. Phys.* **2015**, *142*, 244101.

(22) Ljungberg, M. P.; Koval, P.; Ferrari, F.; Foerster, D.; Sánchez-Portal, D. Cubic-scaling iterative solution of the Bethe-Salpeter equation for finite systems. *Phys. Rev. B: Condens. Matter Mater. Phys.* **2015**, *92*, 075422.

(23) Blase, X.; Boulanger, P.; Bruneval, F.; Fernandez-Serra, M.; Duchemin, I. GW and Bethe-Salpeter study of small water clusters. *J. Chem. Phys.* **2016**, *144*, 034109.

(24) Rangel, T.; Hamed, S. M.; Bruneval, F.; Neaton, J. B. An assessment of low-lying excitation energies and triplet instabilities of organic molecules with an ab initio Bethe-Salpeter equation approach and the Tamm-Dancoff approximation. *J. Chem. Phys.* **2017**, *146*, 194108.

(25) Blase, X.; Duchemin, I.; Jacquemin, D. The Bethe−Salpeter equation in chemistry: relations with TD-DFT, applications and challenges. *Chem. Soc. Rev.* **2018**, *47*, 1022−1043.

(26) Fetter, A. L.; Walecka, J. D. *Quantum Theory of Many-Particle Systems*; McGraw−Hill: New York, 1971.

(27) Parr, R. G.; Yang, W. *Density-Functional Theory of Atoms and Molecules*; Oxford University Press: New York, 1989.

(28) Cederbaum, L. S. One-body Green's function for atoms and molecules: theory and application. *J. Phys. B: At. Mol. Phys.* **1975**, *8*, 290.

(29) Hybertsen, M. S.; Louie, S. G. Electron correlation in semiconductors and insulators: Band gaps and quasiparticle energies. *Phys. Rev. B: Condens. Matter Mater. Phys.* **1986**, *34*, 5390−5413.

(30) van Schilfgaarde, M.; Kotani, T.; Faleev, S. Quasiparticle Self-Consistent GW Theory. *Phys. Rev. Lett.* **2006**, *96*, 226402.

(31) Caruso, F.; Rinke, P.; Ren, X.; Scheffler, M.; Rubio, A. Unified description of ground and excited states of finite systems: The self-consistent GW approach. *Phys. Rev. B: Condens. Matter Mater. Phys.* **2012**, *86*, 081102.

(32) Godby, R. W.; Schlüter, M.; Sham, L. J. Accurate Exchange-Correlation Potential for Silicon and Its Discontinuity on Addition of an Electron. *Phys. Rev. Lett.* **1986**, *56*, 2415−2418.

DOI: 10.1021/acs.jctc.9b00333
J. Chem. Theory Comput. 2019, 15, 4069−4078

(33) Ramberger, B.; Schäfer, T.; Kresse, G. Analytic Interatomic Forces in the Random Phase Approximation. *Phys. Rev. Lett.* **2017**, *118*, 106403.
(34) Bruneval, F. Improved density matrices for accurate molecular ionization potentials. *Phys. Rev. B: Condens. Matter Mater. Phys.* **2019**, *99*, 041118.
(35) Møller, C.; Plesset, M. S. Note on an Approximation Treatment for Many-Electron Systems. *Phys. Rev.* **1934**, *46*, 618−622.
(36) Bartlett, R. J.; Musiał, M. Coupled-cluster theory in quantum chemistry. *Rev. Mod. Phys.* **2007**, *79*, 291−352.
(37) Sham, L. J.; Schlüter, M. Density-Functional Theory of the Energy Gap. *Phys. Rev. Lett.* **1983**, *51*, 1888−1891.
(38) Niquet, Y. M.; Fuchs, M.; Gonze, X. Exchange-correlation potentials in the adiabatic connection fluctuation-dissipation framework. *Phys. Rev. A: At., Mol., Opt. Phys.* **2003**, *68*, 032507.
(39) Helgaker, T.; Jørgensen, P.; Olsen, J. *Molecular Electronic Structure Theory*; John Wiley & Sons, Ltd.: Chichester, U.K., 2000.
(40) Bruneval, F.; Rangel, T.; Hamed, S. M.; Shao, M.; Yang, C.; Neaton, J. B. molgw 1: Many-body perturbation theory software for atoms, molecules, and clusters. *Comput. Phys. Commun.* **2016**, *208*, 149−161.
(41) Tiago, M. L.; Chelikowsky, J. R. Optical excitations in organic molecules, clusters, and defects studied by first-principles Green's function methods. *Phys. Rev. B: Condens. Matter Mater. Phys.* **2006**, *73*, 205334.
(42) Casida, M. E. In *Recent Advances in Density Functional Methods, Part I*; Chong, D., Ed.; World Scientific: Singapore, 1995; pp 155.
(43) Shirley, E. L.; Martin, R. M. GW quasiparticle calculations in atoms. *Phys. Rev. B: Condens. Matter Mater. Phys.* **1993**, *47*, 15404−15412.
(44) van Setten, M. J.; Weigend, F.; Evers, F. The GW-Method for Quantum Chemistry Applications: Theory and Implementation. *J. Chem. Theory Comput.* **2013**, *9*, 232−246.
(45) Rojas, H. N.; Godby, R. W.; Needs, R. J. Space-Time Method for *Ab Initio* Calculations of Self-Energies and Dielectric Response Functions of Solids. *Phys. Rev. Lett.* **1995**, *74*, 1827−1830.
(46) Szabó, A.; Ostlund, N. S. *Modern Quantum Chemistry: Introduction to Advanced Electronic Structure Theory*; Dover Publications: Mineola, NY, 1996.
(47) Ren, X.; Tkatchenko, A.; Rinke, P.; Scheffler, M. Beyond the Random-Phase Approximation for the Electron Correlation Energy: The Importance of Single Excitations. *Phys. Rev. Lett.* **2011**, *106*, 153003.
(48) Dunning, T. H. Gaussian basis sets for use in correlated molecular calculations. I. The atoms boron through neon and hydrogen. *J. Chem. Phys.* **1989**, *90*, 1007−1023.
(49) Weigend, F.; Köhn, A.; Hättig, C. Efficient use of the correlation consistent basis sets in resolution of the identity MP2 calculations. *J. Chem. Phys.* **2002**, *116*, 3175−3183.
(50) Frisch, M. J.; Trucks, G. W.; Schlegel, H. B.; Scuseria, G. E.; Robb, M. A.; Cheeseman, J. R.; Scalmani, G.; Barone, V.; Petersson, G. A.; Nakatsuji, H.; Li, X.; Caricato, M.; Marenich, A. V.; Bloino, J.; Janesko, B. G.; Gomperts, R.; Mennucci, B.; Hratchian, H. P.; Ortiz, J. V.; Izmaylov, A. F.; Sonnenberg, J. L.; Williams-Young, D.; Ding, F.; Lipparini, F.; Egidi, F.; Goings, J.; Peng, B.; Petrone, A.; Henderson, T.; Ranasinghe, D.; Zakrzewski, V. G.; Gao, J.; Rega, N.; Zheng, G.; Liang, W.; Hada, M.; Ehara, M.; Toyota, K.; Fukuda, R.; Hasegawa, J.; Ishida, M.; Nakajima, T.; Honda, Y.; Kitao, O.; Nakai, H.; Vreven, T.; Throssell, K.; Montgomery, J. A., Jr.; Peralta, J. E.; Ogliaro, F.; Bearpark, M. J.; Heyd, J. J.; Brothers, E. N.; Kudin, K. N.; Staroverov, V. N.; Keith, T. A.; Kobayashi, R.; Normand, J.; Raghavachari, K.; Rendell, A. P.; Burant, J. C.; Iyengar, S. S.; Tomasi, J.; Cossi, M.; Millam, J. M.; Klene, M.; Adamo, C.; Cammi, R.; Ochterski, J. W.; Martin, R. L.; Morokuma, K.; Farkas, O.; Foresman, J. B.; Fox, D. J. *Gaussian16, Revision B.01*; Gaussian, Inc.: Wallingford, CT, 2016.
(51) Perdew, J. P.; Burke, K.; Ernzerhof, M. Generalized Gradient Approximation Made Simple. *Phys. Rev. Lett.* **1996**, *77*, 3865−3868.
(52) Adamo, C.; Barone, V. Toward reliable density functional methods without adjustable parameters: The PBE0 model. *J. Chem. Phys.* **1999**, *110*, 6158−6170.
(53) Caruso, F.; Dauth, M.; van Setten, M. J.; Rinke, P. Benchmark of GW Approaches for the GW100 Test Set. *J. Chem. Theory Comput.* **2016**, *12*, 5076−5087.
(54) Stan, A.; Dahlen, N. E.; van Leeuwen, R. Levels of self-consistency in the GW approximation. *J. Chem. Phys.* **2009**, *130*, 114105.
(55) Almbladh, C.-O.; Barth, U. V.; Leeuwen, R. V. Variational Total Energies from Φ- and Ψ- Derivable Theories. *Int. J. Mod. Phys. B* **1999**, *13*, 535−541.
(56) Dahlen, N. E.; van Leeuwen, R.; von Barth, U. Variational energy functionals of the Green function and of the density tested on molecules. *Phys. Rev. A: At., Mol., Opt. Phys.* **2006**, *73*, 012511.
(57) Hellgren, M.; Caruso, F.; Rohr, D. R.; Ren, X.; Rubio, A.; Scheffler, M.; Rinke, P. Static correlation and electron localization in molecular dimers from the self-consistent RPA and GW approximation. *Phys. Rev. B: Condens. Matter Mater. Phys.* **2015**, *91*, 165110.
(58) Galitskii, V. M.; Migdal, A. B. Application of quantum field theory methods to the many body problem. *Sov. Phys. JETP* **1958**, *139*, 96.
(59) Klein, A. Perturbation Theory for an Infinite Medium of Fermions. II. *Phys. Rev.* **1961**, *121*, 950−956.
(60) Pines, D.; Nozières, P. *Theory of Quantum Liquids*; W. A. Benjamin: New York, 1966.
(61) Luttinger, J. M.; Ward, J. C. Ground-State Energy of a Many-Fermion System. II. *Phys. Rev.* **1960**, *118*, 1417−1427.
(62) Dahlen, N. E.; von Barth, U. Variational second-order Møller-Plesset theory based on the Luttinger-Ward functional. *J. Chem. Phys.* **2004**, *120*, 6826−6831.
(63) Dahlen, N. E.; von Barth, U. Variational energy functionals tested on atoms. *Phys. Rev. B: Condens. Matter Mater. Phys.* **2004**, *69*, 195102.
(64) Furche, F. Molecular tests of the random phase approximation to the exchange-correlation energy functional. *Phys. Rev. B: Condens. Matter Mater. Phys.* **2001**, *64*, 195120.
(65) Fuchs, M.; Gonze, X. Accurate density functionals: Approaches using the adiabatic-connection fluctuation-dissipation theorem. *Phys. Rev. B: Condens. Matter Mater. Phys.* **2002**, *65*, 235109.
(66) Scuseria, G. E.; Henderson, T. M.; Sorensen, D. C. The ground state correlation energy of the random phase approximation from a ring coupled cluster doubles approach. *J. Chem. Phys.* **2008**, *129*, 231101.
(67) Bruneval, F. Range-Separated Approach to the RPA Correlation Applied to the van der Waals Bond and to Diffusion of Defects. *Phys. Rev. Lett.* **2012**, *108*, 256403.
(68) Grabowski, B.; Wippermann, S.; Glensk, A.; Hickel, T.; Neugebauer, J. Random phase approximation up to the melting point: Impact of anharmonicity and nonlocal many-body effects on the thermodynamics of Au. *Phys. Rev. B: Condens. Matter Mater. Phys.* **2015**, *91*, 201103.
(69) Dorner, F.; Sukurma, Z.; Dellago, C.; Kresse, G. Melting Si: Beyond Density Functional Theory. *Phys. Rev. Lett.* **2018**, *121*, 195701.
(70) Niquet, Y. M.; Gonze, X. Band-gap energy in the random-phase approximation to density-functional theory. *Phys. Rev. B: Condens. Matter Mater. Phys.* **2004**, *70*, 245115.
(71) Schindlmayr, A.; García-González, P.; Godby, R. W. Diagrammatic self-energy approximations and the total particle number. *Phys. Rev. B: Condens. Matter Mater. Phys.* **2001**, *64*, 235106.
(72) Handy, N. C.; Schaefer, H. F. On the evaluation of analytic energy derivatives for correlated wave functions. *J. Chem. Phys.* **1984**, *81*, 5031−5033.
(73) Hättig, C.; Hellweg, A.; Köhn, A. Distributed memory parallel implementation of energies and gradients for second-order Møller−Plesset perturbation theory with the resolution-of-the-identity approximation. *Phys. Chem. Chem. Phys.* **2006**, *8*, 1159−1169.
(74) Rybkin, V. V.; VandeVondele, J. Spin-Unrestricted Second-Order Mø ller−Plesset (MP2) Forces for the Condensed Phase: From Molecular Radicals to F-Centers in Solids. *J. Chem. Theory Comput.* **2016**, *12*, 2214−2223.

DOI: 10.1021/acs.jctc.9b00333
J. Chem. Theory Comput. 2019, 15, 4069−4078

(75) Faleev, S. V.; van Schilfgaarde, M.; Kotani, T. All-Electron Self-Consistent GW Approximation: Application to Si, MnO, and NiO. *Phys. Rev. Lett.* **2004**, *93*, 126406.
(76) Bruneval, F.; Gatti, M. In *First Principles Approaches to Spectroscopic Properties of Complex Materials*; Di Valentin, C., Botti, S., Cococcioni, M., Eds.; Topics in Current Chemistry, Vol. *347*; Springer: Berlin, Heidelberg, 2014; pp 99−136.
(77) Bruneval, F.; Vast, N.; Reining, L. Effect of self-consistency on quasiparticles in solids. *Phys. Rev. B: Condens. Matter Mater. Phys.* **2006**, *74*, 045102.
(78) Shishkin, M.; Kresse, G. Self-consistent GW calculations for semiconductors and insulators. *Phys. Rev. B: Condens. Matter Mater. Phys.* **2007**, *75*, 235102.
(79) Cunningham, B.; Grüning, M.; Azarhoosh, P.; Pashov, D.; van Schilfgaarde, M. Effect of ladder diagrams on optical absorption spectra in a quasiparticle self-consistent GW framework. *Phys. Rev. Materials* **2018**, *2*, 034603.
(80) Bruneval, F. GW Approximation of the Many-Body Problem and Changes in the Particle Number. *Phys. Rev. Lett.* **2009**, *103*, 176403.
(81) Kaplan, F.; Harding, M. E.; Seiler, C.; Weigend, F.; Evers, F.; van Setten, M. J. Quasi-Particle Self-Consistent GW for Molecules. *J. Chem. Theory Comput.* **2016**, *12*, 2528−2541.
(82) Véril, M.; Romaniello, P.; Berger, J. A.; Loos, P.-F. Unphysical Discontinuities in GW Methods. *J. Chem. Theory Comput.* **2018**, *14*, 5220−5228.

DOI: 10.1021/acs.jctc.9b00333
J. Chem. Theory Comput. 2019, 15, 4069−4078